

Title	Formation of Ce ³⁺ at the cerium dioxide (110) surface by doping
Authors	Nolan, Michael
Publication date	2010-04-24
Original Citation	Nolan, M. (2010) 'Formation of Ce ³⁺ at the cerium dioxide (110) surface by doping', Chemical Physics Letters, 492(1), pp. 115-118. doi: 10.1016/j.cplett.2010.04.035
Type of publication	Article (peer-reviewed)
Link to publisher's version	http://www.sciencedirect.com/science/article/pii/S0009261410005580 - 10.1016/j.cplett.2010.04.035
Rights	© 2010 Elsevier B.V. This manuscript version is made available under the CC-BY-NC-ND 4.0 license - http://creativecommons.org/licenses/by-nc-nd/4.0/
Download date	2023-05-04 16:14:58
Item downloaded from	http://hdl.handle.net/10468/5193

Formation of Ce^{3+} at the Cerium Dioxide (110) surface by Doping

Michael Nolan

Tyndall National Institute, Lee Maltings, University College Cork, Lee Maltings, Prospect

Row, Cork, Ireland

michael.nolan@tyndall.ie

Abstract

The formation of Ce^{3+} ions in CeO_2 is key for its applications. We present density functional theory (DFT) studies of doping of the CeO_2 (110) surface with +5 cations, Ta and Nb, as a route to formation of Ce^{3+} . We use DFT corrected for on-site Coulomb interactions (DFT+U, $U = 5$ eV) and hybrid DFT (HSE06 functional). With both methods we find formation of Ce^{3+} ions due to the extra electron from the dopant residing on a single Ce site, confirming the DFT+U description of these systems. We find that doping with Nb and Ta activates the surface to NO_2 reduction - there is no interaction with the undoped surface and the Ce^{3+} ion in the doped surface interacts strongly with NO_2 .

Introduction

Ceria is a widely used metal oxide in catalytic applications, for CO oxidation and NO_x reduction [1, 2]. This utility arises from the relative ease with which Ce^{4+} can be reduced to Ce^{3+} through, e.g. oxygen vacancy formation [3, 4]. The loss of oxygen facilitates CO oxidation [5 - 7], while the reduced Ce^{3+} remaining at the surface are active sites for adsorption of NO_x [8], and the ultimate reduction to N_2 .

There has been a great deal of interest in doping ceria to enhance its reactivity, with a particular focus on CO oxidation [2, 6, 9, 10]. Substitutional cation doping of ceria with

another species, such as Zr [10 - 12], Ti [10], Au [6] and Cu [13], has been shown to reduce the energy required for formation of oxygen vacancies.

However, less attention has been given to NO_x reduction. It is known that NO_x reduction requires Ce³⁺ sites to be present [14] and earlier modelling work has studied the adsorption of NO₂ at reduced ceria surfaces [8, 15]. We are interested in systems in which Ce³⁺ can be produced by doping, in addition to oxygen vacancy formation. To this end, we present a first principles study of the Ta and Nb doped CeO₂ (110) surface. Work from Ramirez-Cabrera *et al* [16] indicates formation of Ce³⁺ upon doping of CeO₂ with Nb and therefore for Nb/Ta doped CeO₂, we expect that one Ce³⁺ ion will be formed. For comparison, a number of papers have shown that doping of TiO₂ with Ta and Nb produces a single reduced Ti³⁺ cation [17].

Given the problems with using density functional theory (DFT) to study ceria, we apply in this paper two DFT approaches are: DFT corrected for on-site Coulomb interactions, DFT+*U* [18] and hybrid DFT, in the shape of the HSE06 functional [19]. While the DFT+*U* approach has been successfully used to describe undoped and doped ceria and its reactivity, as evidenced in a number of publications [3 – 5, 7 – 10, 12, 20 - 24], it suffers from the need for a choice of *U* parameter. Hybrid DFT has been used to describe successfully the oxygen vacancy in the (111) ceria surface [25], but is a very expensive approach for studies of systems with a large number of atoms, placing a limit on the type of systems that can be studied.

Our approach is the following: we use DFT+*U* (*U* = 5 eV [3]) and HSE06 to study the Ta and Nb doped (110) surface and show that DFT+*U* provides a consistent description of the resulting Ce³⁺ defect, with one Ce³⁺ ion being formed. We then use DFT+*U* to study NO₂ adsorption at the doped surface. The choice of *U* in the present paper is sufficient to describe localised Ce³⁺ and is used throughout. We show that at the undoped surface, NO₂ does not

react, but NO_2 reacts with the Ce^{3+} present at the doped surface, showing that Ce^{3+} species are needed to activate NO_2 .

Methods

We use slab models of the surfaces and a plane wave basis set to describe the valence electronic wave functions with the VASP code [26]. The cut-off for the kinetic energy is 396 eV. For the core-valence interaction we apply Blöchl's projector augmented wave (PAW) approach [27]. For Ce, we use 12 valence electrons, for Nb 11 valence electrons, Ta 5 valence electrons and for O and N six and five valence electrons, respectively. We use the Perdew-Burke-Ernzerhof (PBE) approximation for the exchange-correlation functional [28]. In common with earlier studies [7 – 10, 12, 20 - 24], we use density functional theory (DFT) corrected for on-site Coulomb interactions (DFT+ U), where $U = 5$ eV and is applied to the Ce $4f$ states in oxidised and reduced ceria, both undoped and doped. The details of this approach and our choice of U are discussed extensively in [3, 4]. The choice of U is an important question. Our choice of $U = 5$ eV was motivated by consistently describing the Ce^{3+} derived state found upon oxygen vacancy formation in reduced ceria [3], where this value resulted in a localised defect state and formation of two Ce^{3+} ions. In a recent paper Huang and Fabris [7] have determined that in order to best match the experimentally determined adsorption energy of CO on ceria U must be set to 2 eV. However, we and others [24], have found that $U = 2$ eV does not describe the electronic structure of Ce^{3+} correctly. This means that while the energy of CO adsorption at ceria might be consistent with experiment, the nature of the reduced Ce^{3+} species will not be consistently described. In earlier work on doping the CeO_2 (110) surface with Ti, Zr and Hf [10], we instead focussed on assessing trends in adsorption energies on going from the undoped to the doped surface and this strategy has also been discussed in ref. [24] and is used in the present paper. To provide a benchmark for the DFT+ U description of

the Ta and Nb doped surface, we also apply the hybrid HSE06 functional, which has been used for oxygen vacancies in the (111) surface [25].

The (110) surface is type I (in the Tasker classification) with each plane made up of stoichiometric CeO₂ layers and no dipole moment is present upon cleaving. We use a (2x2) expansion of the (110) surface supercell [10], giving a dopant concentration of 3.6 % and from ref. [3] the slab thickness is 7 layers (11.5 Å), with a 15 Å vacuum gap. The bottom two layers were fixed during the relaxations. All calculations are spin polarised. k-point sampling is performed using the Monkhorst-Pack scheme, with a (2x2x1) sampling grid, suitable for this surface expansion [3].

The adsorption energy of NO₂ is given by

$$E^{\text{ads}} = E(\text{M}_{0.036}\text{Ce}_{1.964}\text{O}_2\text{-NO}_2) - [E(\text{M}_{0.036}\text{Ce}_{1.964}\text{O}_2) + E(\text{NO}_2)] \quad (1)$$

In eqn (1), the dopant concentrations are given in the subscripts on Ce and M (M = Ta, Nb).

For undoped ceria the concentration of M is zero. Throughout, a negative energy signifies that formation of adsorbed NO₂ is favourable.

Results

The Doped (110) Surface

In figure 1 we show the structure of the (110) ceria surface doped with Ta (figure 1(a)) and Nb (figure 1(b)) from the HSE06 calculations (the DFT+U picture is little changed). It is immediately apparent that doping with Ta introduces substantial distortions to the local atomic structure around the dopant, while distortions with Nb doping are less strong.

In the undoped (110) surface, surface Ce ions are coordinated to four oxygen atoms in the surface layer and two oxygen atoms in the next subsurface layer, with Ce-O distances of 2.33 Å. With Ta doping, there are now three shorter surface Ta-O distances in both DFT+U and

HSE06, as shown in table 1 and a very long Ta-O distance of 3.53 Å, so that Ta only coordinates to 3 surface Ce ions. Also, one surface oxygen atom is pushed out of the surface plane by 0.80 Å. Ta-O distances to the two subsurface oxygen ions are 1.98 Å. In terms of Ce, there are changes in the environment of Ce nearest the dopant, with a short surface Ce-O distance of 1.94 Å and two other Ce-O distances 2.25 and 2.39 Å. The fourth surface oxygen is the oxygen that now protrudes from the surface.

With Nb doping, the distortions around the dopant are less strong resulting in more uniform Nb-O distances when compared to Ta doping, although the dopant sinks towards the bulk, by 0.36 Å. The 4 surface Nb-O distances are found in two pairs with both DFT approaches, all of which are shorter than in the undoped surface, with oxygen neighbouring the dopant. The Ce ion nearest the dopant shows four elongated Ce-O distances, in the range 2.50 – 2.72 Å, consistent with the short dopant-O distances in the surface.

Thus DFT+U and HSE06 give similar structural changes upon doping of the ceria surface with Ta and Nb.

Since the dopants have a formal +5 oxidation state, the ionic picture says that four of the electrons will be donated to oxygen, with one electron left to be accommodated. In fact, this question is similar to the case of Ta and Nb doped TiO₂, which has been recently studied for transparent conducting oxide applications [17]. To see the destination of the extra electron, we plot in figure 2 the spin density of that electron for both dopants from HSE06, with the DFT+U results being the same. The spin density for the surface with both dopants shows that the extra electron is transferred to a surface Ce ion, which is consequently reduced from Ce⁴⁺ to Ce³⁺. The spin density isosurface is characteristic of a 4*f* orbital, consistent with earlier studies and irrespective of the DFT method used. This Ce ion shows the elongated Ce-O distances discussed above, e.g. for Nb, consistent with it being in a reduced state.

The dopants give different lattice sites for the Ce^{3+} ion and we attribute this to the different structural distortions that occur for each dopant – e.g. the Ce ion nearest the Ta is unable to accommodate the extra electron in its distorted environment. Recent work has shown for the (111) surface that the site at which Ce^{3+} ions are found is influenced by the distortions to the structure that occur, as discussed in recent work [25, 29].

Figure 3 shows the total electronic density of states (EDOS) for the (110) surface with both dopants from DFT+U and HSE06. Both methods result in formation of a $\text{Ce}4f$ state in the previously energy gap between the top of the valence band and the unoccupied Ce $4f$ states. However, there are differences in the positions of the $\text{Ce}4f$ state between the dopants and between the DFT approaches. For Nb, DFT+U places the $\text{Ce}4f$ state very close to the top of the VB, while HSE06 positions this state 1.5 eV above the valence band edge. For Ta doping, the offset from the valence band edge to the gap state is 1.5 eV with DFT+U and 2.2 eV with HSE06. Thus, the differences between the position of the $\text{Ce}4f$ gap state with each dopant are consistent from DFT+U and HSE06, and the band gap underestimation in DFT+U does impact on the precise position of the $\text{Ce}4f$ states in the band gap.

Adsorption of NO_2 at the Doped (110) Surface

The formation of Ce^{3+} upon doping provides a reactive site for adsorption of NO_2 , which is a key step in the reduction of NO_2 to N_2 . We have already shown using DFT+U ($U = 5$ eV on Ce, as in the present paper) [8] that NO_2 adsorbs strongly at undoped ceria surfaces in which Ce^{3+} forms upon oxygen vacancy formation. One of these Ce^{3+} is reoxidised to Ce^{4+} and NO_2 is partially reduced to an $[\text{NO}_2]^-$ anion. Experimental work indicates that NO_2 will not adsorb at non-defective ceria (111) surface [14], but there are no available experimental data for the energetics of adsorption at undoped or doped surfaces (whether with or without oxygen vacancies). With DFT+U giving a consistent description of the formation of Ce^{3+} from Ta and

NB doping, we have carried out a DFT+*U* calculation of NO₂ adsorption at the defect-free, undoped (110) surface and find no interaction between the molecule and the oxide.

We initially adsorb NO₂ at the (110) surface with Ta and Nb dopants and position one oxygen atom over the surface Ce³⁺ ion and relax using DFT+*U*. We found that in ref. [8] one oxygen atom of NO₂ interacts with surface Ce³⁺, so that this is a reasonable starting point. We have tried different adsorption configurations and those presented in this paper were the most stable. The final adsorption structures are shown in figure 3. The adsorption energies show a gain of −0.87 eV (Ta) and −0.73 eV (Nb), indicating favourable adsorption of NO₂ and a reasonably strong interaction.

On the doped surfaces, one oxygen from NO₂ (denoted O_S) coordinates to the surface Ce³⁺ ion, with Ce-O_S distances of 2.23 Å (Ta) and 2.21 Å (Nb). The N-O_S distances are 1.37 Å (Ta) and 1.38 Å (Nb), while the N-O distance to the other oxygen of NO₂ (denoted O_N) is 1.21 Å at both surfaces. For comparison, at the undoped (110) surface [8], we found an N-O_S distance of 1.31 Å and an N-O_N distance of 1.25 Å. Thus at Ta and Nb doped surfaces, NO₂ is activated by interaction with the Ce³⁺ ion. This results in an elongation of the N-O_S distance, with the N-O_N distance little changed from the N-O distance in free NO. This means that the NO₂ molecule is dissociating to oxygen and NO (which can undergo further reduction to N₂).

An analysis of the electronic structure shows that the Ce 4*f* electron initially in the Ce³⁺ species is transferred to the NO₂ molecule, which is now an [NO₂][−] anion. This mechanism of Ce³⁺-to-adsorbate charge transfer is the same as that which was elucidated for NO₂ adsorption at the undoped surface with oxygen vacancies [8]. Thus the vital factor in the reduction of NO₂ is the presence of Ce³⁺ ions at the oxide surface and the ease with which such ions can be reoxidised through charge transfer to an adsorbate. Doping of ceria with high oxidation state cations is a novel and potentially more controlled means of generating Ce³⁺ ions that are active for molecular reduction, as compared to oxygen vacancy formation.

Summary

It is usual to think of Ce^{3+} ions in ceria as being formed by oxygen vacancies. We compare two density functional theory approaches, DFT+U and hybrid HSE06, to demonstrate that Ce^{3+} ions are produced by substitutional doping of CeO_2 with +5 cations, Ta and Nb. This strategy should be a more controlled means of introducing Ce^{3+} ions, with one such ion formed for each +5 dopant. We also show that at these doped surfaces, the presence of the Ce^{3+} ions is key to activating NO_2 , by charge transfer from Ce^{3+} to the molecule, which weakens one NO bond and is the first step in dissociation to NO and oxygen.

Supporting Information

Results from DFT+U calculations for Ta and Nb doped CeO_2 (110) surface are shown

Acknowledgements

We acknowledge support from Science Foundation Ireland through the Starting Investigator Grant Program (EMOIN, 09/SIRG/I1620). We acknowledge a generous grant of computer time at Tyndall from Science Foundation Ireland, and the SFI/Higher Education Authority funded Irish Centre for High End Computing (ICHEC) for the generous provision of computational facilities.

References

1. A. Trovarelli, *Catalysis by Ceria and Related Materials*, Imperial College Press, London, UK, 2002

2. A. Trovarelli, *Catalysis Reviews – Science and Engineering*, 38 (1996) 439
- 3 M. Nolan, S. Grigoleit, D. C. Sayle, S. C. Parker, S. C. and G. W. Watson, *Surf. Sci.* 576 (2005) 217
4. M. Nolan, S. C. Parker and G. W. Watson, *Surf. Sci.* 595 (2005) 223
5. M. Nolan, and G. W. Watson, *J. Phys. Chem. B*, 110 (2006) 16600
6. V. Shapovalov and H. Metiu, *J. Cat.* 245 (2007) 205
7. M. Huang, and S. Fabris, *J. Phys. Chem C*, 112 (2008) 8643
8. M. Nolan, S. C. Parker and G. W. Watson, *J. Phys. Chem B*, 110 (2006) 2256
9. M. Nolan, V. Soto Verdugo V and H. Metiu, *Surf. Sci.* 602 (2008) 2734
10. M. Nolan, *J. Phys. Chem C*, 113 (2009) 2425
11. G. Balducci, M. S. Islam, J. Kaspar, P. Fornasiero, and M. Graziani, *Chem Mat.*, 12 (2000) 677
12. Z. Yang, T. K. Woo, and K. Hermansson, *J. Chem. Phys.*, 124 (2006) 224704
13. J. A. Rodriguez, T. Jirsak, A. Freitag, J. C. Hanson, J. Z. Larase and S. Chaturvedi, *Cat. Lett.*, 62 (1999) 113
14. Y. Namai, K. Fukui and Y. Iwasawa, *Nanotechnology* 15 (2004) S49
15. M. Nolan, *J. Chem. Phys.*, 130 (2009) 144702
16. E. Ramirez-Cabrera, A. Atkinson and D. Chadwick, *Appl. Cat. B*, 36 (2002) 193
17. B. J. Morgan, D. O. Scanlon and G. W. Watson, *J. Mat. Chem*, 10 (2009) 5175
18. S. L. Dudarev, G. A. Botton, S. Y. Savrasov, C. J. Humphreys and A. P. Sutton, *Phys. Rev. B* 57 (1998) 1505
19. B. J. Janesko, T. M. Henderson and G. E. Scuseria, *Phys. Chem. Chem. Phys.*, 11 (2009) 443
20. Z. Yang, Y. Wei, Z. Fu, Z. Lu and K. Hermansson., *Surf. Sci.*, 602 (2008) 1199
21. A. Migani, C. Loschen, F. Illas and K. M. Neyman, *Chem. Phys. Lett.*, 465 (2008) 106

22. J. C. Conesa *Catalysis Today*, 143 (2009) 315
23. A. D. Myernick and M. J. Janik, *J. Phys. Chem C*, 112 (2008) 14955
24. Z. Yang, Z. Fu, Y. Wei and Z. Li, *J. Phys. Chem. C*, 112 (2008) 15341
25. M. V. Ganduglia-Pirovano, J. L. F. Da Silva and J. Sauer, *Phys. Rev. Lett.*, 102 (2009) 026101
26. G. Kresse, and J. Hafner, *Phys. Rev. B* 49 (1994) 14251
27. P. E. Blöchl, *Phys. Rev. B* 50 (1994) 17953
28. J. P. Perdew, K. Burke, and M. Ernzerhof, *Phys. Rev. Lett.*, 77 (1996) 3865
29. H. Y. Li, H. F. Wang, X. Q. Gong, Y. L. Guo, Y. Guo, G. Z. Lu and P. Hu, *Phys. Rev. B* 79 (2009) 193401.

Figures

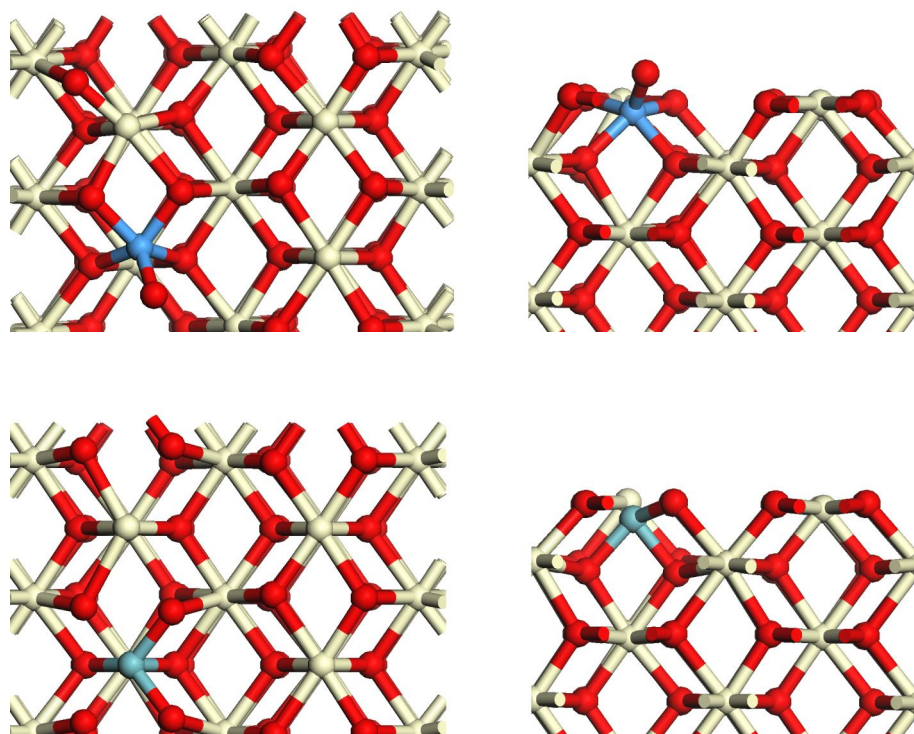


Figure 1: (a): structure of the (110) surface with Ta dopant, (b): structure of the (110) surface with Nb dopant from HSE06. The left hand image in each case shows the plan view of the surface and the right hand image shows a side view of the surface. Throughout, Ce ions are grey, O is red and the dopants are the light blue spheres.

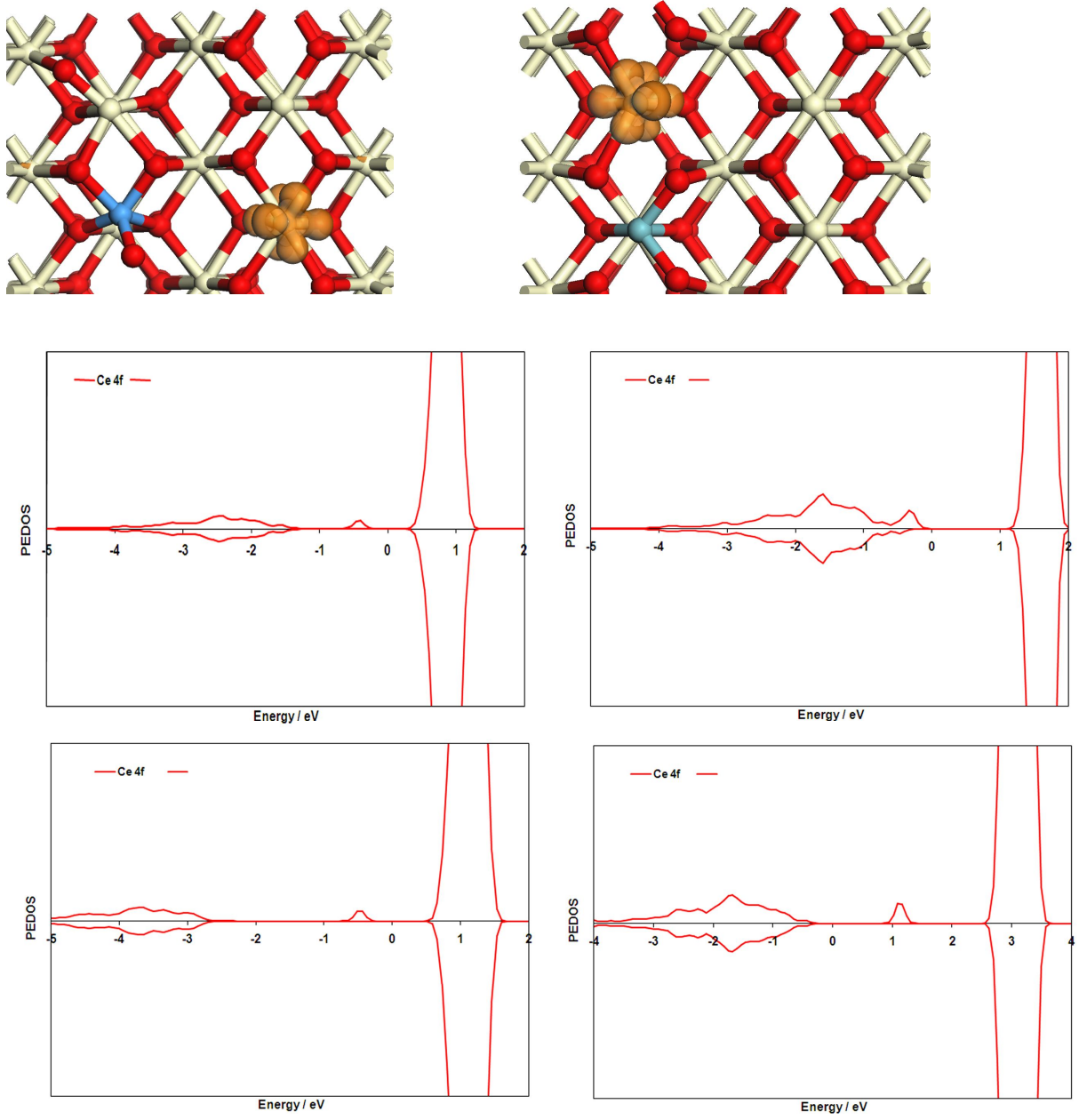


Figure 2: (a): Excess spin density for the (110) surface doped with Ta, (b): Excess spin density for the (110) surface doped with Nb from HSE06. Each image shows the plan view of the surface. (c): Ce 4f projected electronic density of states for doped CeO₂ from DFT+U and HSE06. The spin density isosurfaces are orange and have a value of 0.01 electrons/Å³ and in (c), the Fermi level is set to 0 eV. The colour scheme of figure 1 is used here.

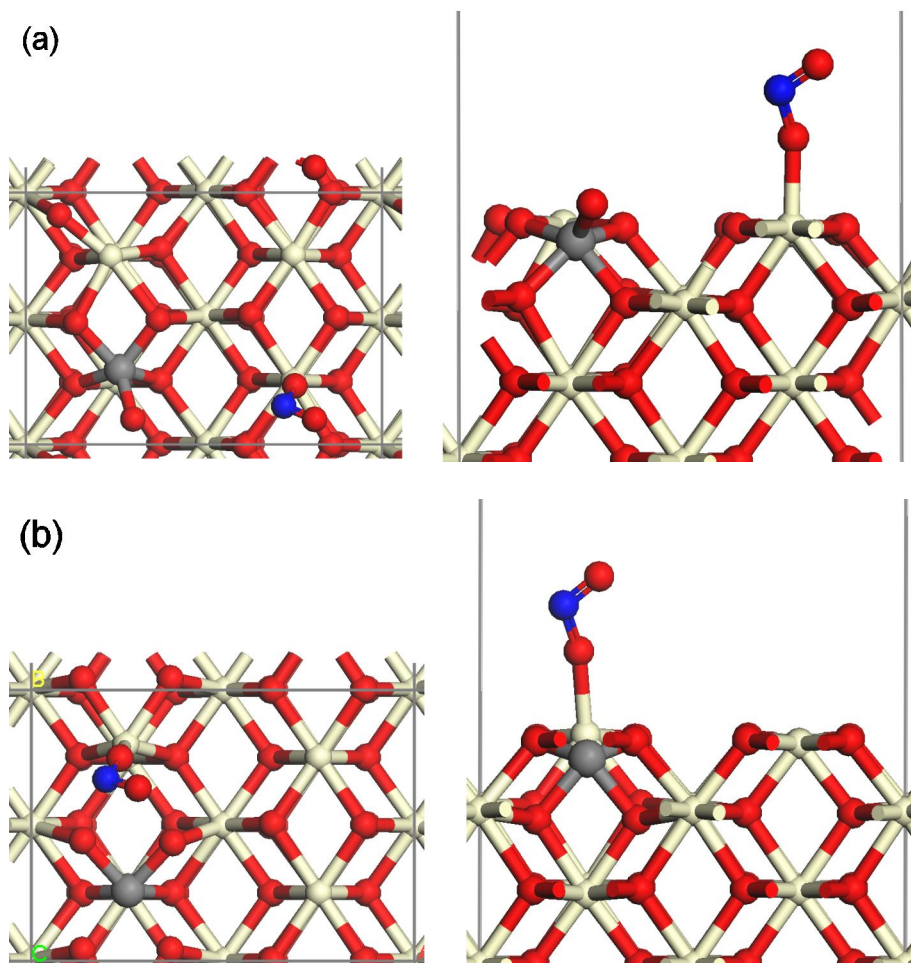


Figure 3: (a): Relaxed structure of NO_2 adsorbed at the Ta-doped (110) surface, (b): Relaxed structure of NO_2 adsorbed at the Nb-doped (110) surface. The left hand image in each case shows the plan view of the surface and the right hand image shows a side view of the surface. The colour scheme of figure 1 is used here and in addition, the dopant is the grey sphere and the N atoms are the blue spheres

Dopant	Ce-O distances (DFT+U) / Å	Ce-O distances (HSE06) / Å
Ta	1.82, 1.96, 2.02, 3.53 (surface Ta-O) 1.98 (subsurface Ta-O)	1.78, 1.98, 2.01, 3.51 (surface Ta-O) 1.98 (subsurface Ta-O)
Nb	2.01, 2.02, 2.14, 2.16 (surface Nb-O) 2.01 (subsurface Nb-O)	1.96, 1.98, 2.17, 2.17 (surface Nb-O) 1.98 (subsurface Nb-O)

Table 1: Dopant-O distances in Ta and Nb doped CeO₂ (110) surface, from DFT+U and HSE06.